Acta Crystallographica Section D
Biological Crystallography
ISSN 0907-4449

Crystallization and preliminary X-ray studies of thymus and activation-regulated chemokine (TARC)

Oluwatoyin A. Asojo,[a] Simon Cater,[a] David M. Hoover,[a] C. Boulègue,[b] Wuyuan Lu[b] and Jacek Lubkowski[a]*

[a]Macromolecular Crystallography Laboratory, National Cancer Institute at Frederick, Frederick, MD 21702, USA, and [b]Institute of Human Virology, University of Maryland Biotechnology Institute, 725 West Lombard Street, Baltimore, MD 21201, USA

Correspondence e-mail: jacek@ncifcrf.gov

Received 1 April 2002
Accepted 14 October 2002

Thymus and activation-regulated chemokine (TARC) is a CC chemokine that is most highly expressed in the thymus. TARC interacts primarily with the CCR4 receptor and to a lesser extent with the CCR8 receptor. Three different crystal forms of synthetically prepared TARC were grown in triclinic, hexagonal and tetragonal systems. The X-ray data for the triclinic crystals (unit-cell parameters $a = 56.46$, $b = 76.48$, $c = 88.37$ Å, $\alpha = 85.8$, $\beta = 72.8$, $\gamma = 70.0^\circ$) extend to 1.85 Å on a conventional radiation source. The hexagonal crystals diffracted to 2.2 Å at a synchrotron-radiation source and belong to either space group $P6_122$ or $P6_522$, with unit-cell parameters $a = 61.8$, $c = 315.$ Å. The tetragonal crystals diffracted to about 5 Å at a synchrotron-radiation source and had approximate unit-cell parameters $a = b = 47.7$, $c = 58.2$ Å.

1. Introduction

Thymus and activation-regulated chemokine (TARC), with the systematic name CCL17, is a typical CC chemokine consisting of 94 amino acids and four conserved cysteine residues. The first 23 residues form a signal peptide. The mature protein has a MW of ~8.0 kDa and a theoretical isoelectric point of 9.7. TARC was initially expressed using an Epstein–Barr virus vector signal sequence trap method and was the first CC chemokine to be shown to be chemotactic for lymphocytes but not for monocytes (Imai *et al.*, 1996, 1997).

TARC interacts specifically with the seven-helical transmembrane G-protein-coupled CCR4 receptor and is highly expressed in the thymus. Lesser expression of TARC is also observed in other tissues, such as the lung, colon and small intestine. TARC also binds to CCR8, giving it an additional role of activation, migration and proliferation of lymphoid cells (Bernardini *et al.*, 1998). The mature TARC protein has 32% amino-acid sequence identity to MDC (CCL22), another CC chemokine that, like TARC, binds to the CCR4 receptor (Godiska *et al.*, 1997). TARC shares a more limited sequence identity with the CC chemokines RANTES, MIP-1β and MCP-3.

TARC is involved in allergy-related diseases including atopic dermatitis (Vestergaard *et al.*, 2001), allergic airway inflammation (Kawasaki *et al.*, 2001) and psoriasis vulgaris (Rottman *et al.*, 2001). TARC is also involved in classic Hodgkin's lymphoma, but not in other varieties of Hodgkin's lymphoma (Peh *et al.*, 2001). TARC binds very tightly to glycosaminoglycans (tighter than either RANTES or MCP-1). This affinity for glycosaminoglycans allows solid-phase gradients of TARC within the extracellular matrix of endothelial cells to attract and immobilize mast-cell granules (Patel *et al.*, 2001). This property causes TARC to attenuate inflammatory responses and may play a role in liver injury after systemic lipopolysaccharide administration (Yoneyama *et al.*, 1998). As a continuation of our efforts in determining the structural basis of the biological properties of chemokines, we have crystallized TARC in several crystal forms.

2. Protein synthesis, folding and purification

The polypeptide chain of TARC was assembled on Boc-Ser(Bzl)-OCH_2-PAM resin by machine-assisted stepwise solid-phase peptide synthesis using the *in situ* DIEA neutralization/HBTU activation protocol developed for Boc chemistry (Schnolzer *et al.*, 1992). After HF cleavage and deprotection, the crude peptide was purified by reversed-phase HPLC and the molecular weight verified by electrospray ionization mass spectrometry (ESI–MS). Oxidative refolding of TARC proceeded quantitatively at 0.5 mg ml^{-1} in 0.2 *M* $NaHCO_3$ containing 2 *M* guanidine hydrochloride, 3 m*M* cysteine and 0.3 m*M* cystine. The final product was purified by HPLC and its molecular weight (8079.0 Da) determined by ESI–MS is in excellent agreement with the expected value (8079.3 Da) calculated based on average isotope compositions.

3. Crystallization

Initial crystallization screens were carried out at three different temperatures, 293, 285 and 277 K, using commercially available sparse-matrix screens. The screens used were Crystal Screen, Crystal Screen II and Crystal Screen Cryo from Hampton Research. Crystals were grown by vapor diffusion in hanging drops which were equilibrated against 1 ml of crystallization solution. Drops were prepared by mixing 2 µl of protein solution (15 mg ml^{-1}) with an equal volume of crystallization solution. All protein solutions for crystallization experiments were obtained by dissolving synthetic TARC in sterile filtered double-distilled water. Initial concentrations were confirmed spectrophotomerically prior to setting up crystallization experiments. Several conditions from Crystal Screen and Crystal Screen Cryo were promising leads that gave small crystals or showers of crystals. The promising lead conditions all had a high salt concentration, notably citrate, acetate and sulfate, an acidic pH between 4.6 and 5.6 and high concentrations of PEG 8000 or 4000. Three different crystal forms belonging to hexagonal, triclinic and tetragonal systems were obtained upon further optimization of these lead conditions.

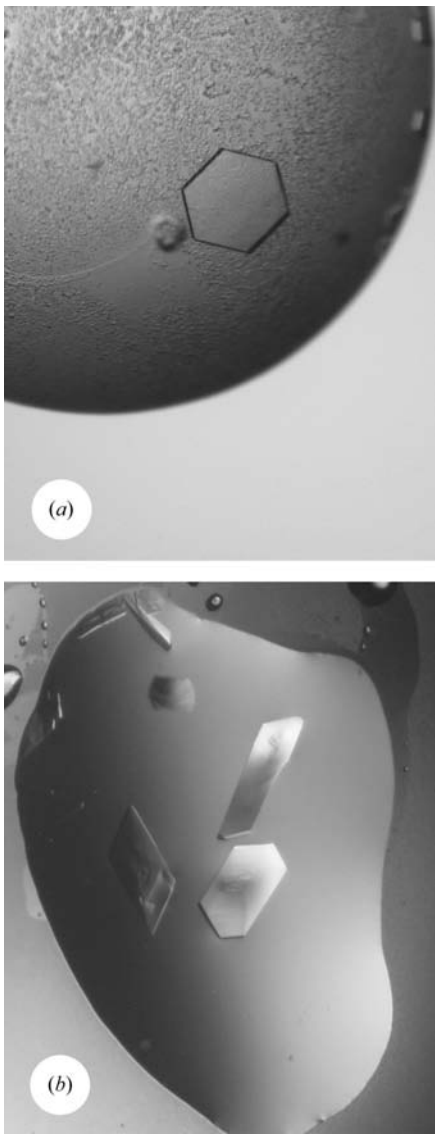

Figure 1
(*a*) A typical hexagonal TARC crystal with approximate crystal dimensions of 0.1 × 0.1 × 0.05 mm. (*b*) Typical TARC triclinic plates come in a variety of shapes and sizes. The largest crystal is in this drop is approximately 0.7 × 0.3 × 0.2 mm.

The crystallization solution for hexagonal crystals contained 400 m*M* lithium sulfate and 15%(*w*/*v*) PEG 8000. 2 µl of protein solution (15 mg ml^{-1}) was mixed with an equal volume of the crystallization solution. Small crystals, less than 0.05 mm on the largest face, were obtained within a few weeks from equilibration of this mixture with the crystallization solution. Diffraction-quality crystals were obtained by macroseeding at 277 K. Macroseeding was achieved by transferring a typical small crystal of almost 0.05 mm on the largest side into a wash solution containing 2 µl of protein solution (15 mg ml^{-1}). After a few minutes, the crystal was transferred into a 4 µl droplet composed of equal volumes of thoroughly mixed protein solution (15 mg ml^{-1}) and crystallization solution. The crystallization solution contained 500 m*M* lithium sulfate, 15%(*w*/*v*) PEG 8000 and 13%(*v*/*v*) glycerol. The plate-like crystal (Fig. 1*a*) reached maximum size after three to four weeks of equilibration against 1 ml of crystallization solution *via* vapor diffusion in hanging drops.

The triclinic crystals grew much faster and reached their maximum size of 0.5 × 0.7 × 0.05 mm within 48 h. These crystals grow by vapor diffusion in hanging drops, which were equilibrated against 1 ml of crystallization solution. Drops were prepared by mixing 1.5 µl of protein solution (40 mg ml^{-1}) with an equal volume of crystallization solution. The crystallization solution contained 0.16 *M* ammonium sulfate, 0.08 *M* sodium acetate trihydrate pH 4.6 as buffer, 20%(*w*/*v*) PEG 4000 as precipitant and 15%(*v*/*v*) glycerol as the cryoprotectant. Crystal growth seemed unaffected by changes in temperature and similar crystals grew at 277, 285 and 293 K. The resulting crystals were thin plates (Fig. 1*b*).

Table 1
X-ray data-collection statistics.

Values in parentheses refer to the highest resolution shells: 2.3–2.20 Å for hexagonal and 1.92–1.85 Å for triclinic crystals.

Data statistics	Hexagonal	Triclinic
Resolution limits (Å)	20–2.2 (2.3–2.2)	20–1.85 (1.92–1.85)
$R_{\rm merge}$†	0.049 (0.411)	0.039 (0.120)
Completeness (%)	100 (100)	93.6 (81.8)
$I/\sigma(I)$	43.1 (5.3)	31.9 (7.65)
Space group	$P6_122$	$P1$
Total No. of reflections	184077	257926
No. of unique reflections	19391 (1866)	53132 (4629)
Redundancy	9.5 (8.0)	4.8 (3.0)

† $R_{\rm merge} = (\sum |I - \langle I \rangle|)/\sum I$, where I is the observed intensity and $\langle I \rangle$ is the average intensity obtained from multiple observations of symmetry-related reflections after rejections.

The tetragonal crystals grew under similar conditions to the triclinic crystals. Long thin needles grew during the equilibration of a 3 µl droplet composed of a mixture of equal volumes of protein solution (15 mg ml^{-1}) and crystallization solution against 1 ml of crystallization solution. The crystallization solution contained 0.2 *M* ammonium acetate, 0.1 *M* sodium acetate trihydrate pH 4.6 and 30%(*w*/*v*) PEG 4000.

4. X-ray diffraction experiments

Prior to flash-freezing in a stream of N_2 at 100 K, a hexagonal crystal was soaked for about 2 min in cryoprotectant solution containing 500 m*M* lithium sulfate, 15%(*w*/*v*) PEG 8000 and 15%(*v*/*v*) glycerol. The crystal was then mounted in a 0.3 mm angled loop and X-ray data were collected on beamline X9B of the National Synchrotron Light Source at Brookhaven. The resolution of the X-ray data extended to 2.2 Å; however, the intensity of the diffraction diminished significantly at a resolution higher that 2.7 Å. Diffraction data were indexed and integrated using *DENZO* (Otwinowski, 1993*a*) and *SCALEPACK* (Otwinowski, 1993*b*). These crystals belong to space group $P6_122$ (or $P6_522$), with unit-cell parameters a = 61.8, c = 315.1 Å. The asymmetric unit is likely to consist of four monomers, assuming a $V_{\rm M}$ (Matthews, 1968) of 2.68 Å^3 Da^{-1} (corresponding to a solvent content of 54%). The most important X-ray statistics are shown in Table 1.

The triclinic crystals could be frozen directly from the crystallization mixture without ice formation. A crystal was simply transferred into a loop and flash-frozen in a stream of N_2. Data were recorded on a MAR 300 detector (MAR Research). The radiation source was a Rigaku RU-200 rotating-anode generator operating at 50 kV and 100 mA, with a double focusing-mirror system. Data were processed using *DENZO*

(Otwinowski, 1993*a*) and *SCALEPACK* (Otwinowski, 1993*b*). Unit-cell parameters were determined as a = 56.46, b = 76.48, c = 88.37 Å, α = 85.8, β = 72.8, γ = 70.0°. Additional statistics for the X-ray data are shown in Table 1. Determination of the contents of the asymmetric unit for this crystal form was more difficult than in the case of hexagonal crystals. Assuming, for instance, 16 molecules per asymmetric unit, V_M is 2.13 Å^3 Da^{-1} (or 54% solvent); however, even significantly fewer molecules in the asymmetric unit results in acceptable solvent contents. It is important to mention that the indexing and data-reduction procedures were performed under numerous conditions (resolution limits, indexing vectors *etc.*) for several X-ray data sets collected from different crystals of the triclinic crystal form. The same unit cell with *P*1 symmetry consistently predicted the locations of all experimental intensities and resulted in complete high-quality data sets, establishing *P*1 as the correct space group, rather than as an artifact arising from poorly diffracting crystals.

The tetragonal crystals were too small for the collection of a suitable X-ray data set. However, long exposures using synchrotron-generated radiation allowed us to determine the approximate unit-cell parameters as $a = b$ = 47.7, c = 58.2 Å. This crystal form would be most suitable for structure determination owing to the small size of the asymmetric unit, but unfortunately we were unable to obtain crystals of higher quality.

5. Dynamic light scattering

Measurements of the dynamic light scattering were performed using a DynaPro DLS Instrument (Protein Solutions, Inc.) for solutions of TARC at concentrations between 10 and 20 mg ml^{-1} buffered with 0.1 *M* sodium acetate pH 4.6. Based on the observed hydrodynamic radii, the approximate molecular weight of the protein was determined as being between 14 and 17 kDa, indicating the formation of a dimeric species. No formation of large molecular-weight aggregates was observed under the measurement conditions.

6. Discussion

Preliminary efforts to solve the structure of TARC in either crystal form by molecular replacement using the structures of other chemokines as search models were unsuccessful. In the case of the hexagonal crystal form, the self-rotation searches did not reveal any significant signal that could correspond to the non-crystallographic symmetry. Such a result is not unusual for chemokines; we have reported similar results previously for MCP-1 (Lubkowski *et al.*, 1997), RANTES (Wilken *et al.*, 1999) and fractalkine (Hoover *et al.*, 2000). In the high-symmetry space groups it is quite likely that non-crystallographic and crystallographic symmetries coincide, therefore effectively masking the presence of the former. In the case of the triclinic crystal form, however, self-rotation searches conducted with both *AMoRe* (Navaza, 1994) and *CNS* (Brünger *et al.*, 1998) showed very strong signals, indicating the presence of three mutually perpendicular twofold axes, one of which coincided with the *b* direction of the unit cell.

Although a tetramer is the native form of platelet factor-4 (St Charles *et al.*, 1989), a member of the CXC chemokine family, proteins from the CC family rarely form tetrameric assemblies (Lubkowski *et al.*, 1997). Moreover, results from the dynamic light-scattering experiments indicated the presence of a dimeric, rather than tetrameric, species in solution. The lack of detectable signal during self-rotation searches with the hexagonal form indicated that the 222 non-crystallographic symmetry detected for the triclinic crystal form might not be associated with the presence of tetramers. Another interesting observation is that only three twofold axes have been found for the triclinic crystal form, while it is clear that the asymmetric unit must contain more than four monomers. It is then quite possible that the arrangement of all monomers satisfies the same 222 symmetry and that the other non-crystallographic symmetries are much weaker and result in undetectable signals during the self-searches.

Using the information from self-rotation searches with caution, we are conducting extensive molecular-replacement searches as well as generating potential heavy-atom derivatives in order to solve the structures of TARC.

We thank Dr Zbigniew Dauter for his help with data collection at beamline X9B, NSLS, Brookhaven National Laboratory. This research was sponsored in part by the Intramural AIDS Targeted Antiviral Program of the Office of the Director, National Institutes of Health (JL).

References

Bernardini, G., Hedrick, J., Sozzani, S., Luini, W., Spinetti, G., Weiss, M., Menon, S., Zlotnik, A., Mantovani, A., Santoni, A. & Napolitano, M. (1998). *Eur. J. Immunol.* **28**, 582–588.

Brünger, A. T., Adams, P. D., Clore, G. M., DeLano, W. L., Gros, P., Grosse-Kunstleve, R. W., Jiang, J. S., Kuszewski, J., Nilges, M., Pannu, N. S., Read, R. J., Rice, L. M., Simonson, T. & Warren, G. L. (1998). *Acta Cryst.* D**54**, 905–921.

Godiska, R., Chantry, D., Raport, C. J., Sozzani, S., Allavena, P., Leviten, D., Mantovani, A. & Gray, P. W. (1997). *J. Exp. Med.* **185**, 1595–1604.

Hoover, D. M., Mizoue, L. S., Handel, T. M. & Lubkowski, J. (2000). *J. Biol. Chem.* **275**, 23187–23193.

Imai, T., Baba, M., Nishimura, M., Kakizaki, M., Takagi, S. & Yoshie, O. (1997). *J. Biol. Chem.* **272**, 15036–15042.

Imai, T., Yoshida, T., Baba, M., Nishimura, M., Kakizaki, M. & Yoshie, O. (1996). *J. Biol. Chem.* **271**, 21514–21521.

Kawasaki, S., Takizawa, H., Yoneyama, H., Nakayama, T., Fujisawa, R., Izumizaki, M., Imai, T., Yoshie, O., Homma, I., Yamamoto, K. & Matsushima, K. (2001). *J. Immunol.* **166**, 2055–2062.

Lubkowski, J., Bujacz, G., Boque, L., Domaille, P. J., Handel, T. M. & Wlodawer, A. (1997). *Nature Struct. Biol.* **4**, 64–69.

Matthews, B. W. (1968). *J. Mol. Biol.* **33**, 491–497.

Navaza, J. (1994). *Acta Cryst.* A**50**, 157–163.

Otwinowski, Z. (1993*a*). *DENZO: An Oscillation Data Processing Program for Macromolecular Crystallography*. New Haven, CT, USA: Yale University Press.

Otwinowski, Z. (1993*b*). *SCALEPACK: Software for the Scaling Together of Integrated Intensities Measured on a Number of Separate Diffraction Images*. New Haven, CT, USA: Yale University Press.

Patel, D. D., Koopmann, W., Imai, T., Whichard, L. P., Yoshie, O. & Krangel, M. S. (2001). *Clin. Immunol.* **99**, 43–52.

Peh, S. C., Kim, L. H. & Poppema, S. (2001). *Am. J. Surg. Pathol.* **25**, 925–929.

Rottman, J. B., Smith, T. L., Ganley, K. G., Kikuchi, T. & Krueger, J. G. (2001). *Lab. Invest.* **81**, 335–347.

St Charles, R., Walz, D. A. & Edwards, B. F. (1989). *J. Biol. Chem.* **264**, 2092–2099.

Schnolzer, M., Alewood, P., Jones, A., Alewood, D. & Kent, S. B. (1992). *Int. J. Pept. Protein Res.* **40**, 180–193.

Vestergaard, C., Kirstejn, N., Gesser, B., Mortensen, J. T., Matsushima, K. & Larsen, C. G. (2001). *J. Dermatol. Sci.* **26**, 46–54.

Wilken, J., Hoover, D., Thompson, D. A., Barlow, P. N., McSparron, H., Picard, L., Wlodawer, A., Lubkowski, J. & Kent, S. B. (1999). *Chem. Biol.* **6**, 43–51.

Yoneyama, H., Harada, A., Imai, T., Baba, M., Yoshie, O., Zhang, Y., Higashi, H., Murai, M., Asakura, H. & Matsushima, K. (1998). *J. Clin. Invest.* **102**, 1933–1941.